

The Galactic Deuterium Abundance and Dust Depletion: Insights From an Expanded Ti/H Sample^{*}

Sara L. Ellison^{1†}, Jason X. Prochaska², Sebastian Lopez³

¹*Dept. Physics & Astronomy, University of Victoria, 3800 Finnerty Rd, Victoria, BC, V8P 1A1, Canada*

²*Dept. of Astronomy and Astrophysics, UCO/Lick Observatory, University of California, 1156 High Street, Santa Cruz, CA 95064, USA*

³*Departamento de Astronomía, Universidad de Chile, Casilla 36-D, Santiago, Chile*

1 February 2008

ABSTRACT

The primordial abundance of deuterium (D/H) yields a measure of the density of baryons in the universe and is an important complement to determinations from cosmic microwave background (CMB) experiments. Indeed, the current small sample of high redshift D/H measurements from quasar absorption line studies are in excellent agreement with CMB-derived values. Conversely, absorption line measurements of the *Galactic* D/H ratio in almost 50 stellar sightlines show a puzzlingly large scatter outside the Local Bubble which is difficult to explain simply by astration from the primordial value. The currently favoured explanation for these large variations is that D is differentially depleted relative to H in some parts of the local interstellar medium (ISM). Here, we test this scenario by studying the correlation between D/H and the abundance of titanium, one of the most refractory elements readily observed in the ISM. Previous work by Prochaska, Tripp & Howk (2005) found tentative evidence for a correlation between Ti/H and D/H based on seven sightlines. Here we almost triple the number of previous Ti measurements and include several sightlines with very high or low D/H that are critical for quantifying any correlations with D/H. With our larger sample, we confirm a correlation between Ti/H and D/H at the 97% confidence level. However, the magnitude of this dependence is difficult to reconcile with a simple model of dust depletion for two reasons. First, contrary to what is expected from local depletion rates, the gradient of the highly refractory Ti is much shallower than that observed for Fe and Si. Second, we do not observe the established tight, steep correlation between [Ti/H] and the mean volume density of hydrogen. Therefore, whilst dust remains a plausible explanation for the local D/H variations, the abundances of at least some of the refractory elements do not provide unanimous support for this scenario. We also argue that the correlations of [Si/H], [Fe/H], and [Ti/H] with D/H are inconsistent with a simple infall model of low metallicity gas with approximately solar abundances as the dominant cause for D variations.

Key words: ISM:abundances, ISM: dust, Galaxy: abundances

1 INTRODUCTION

The abundances of the light elements (deuterium, helium and lithium) form one of the cornerstones of Big Bang nucleosynthesis theory and can all be used as baryometers, yielding the density of baryons in the universe as a fraction of the closure density, Ω_b . Although the light element abundances

are actually a direct probe of the baryon-to-photon ratio, η , this can be translated to Ω_b using the (now well-known) Cosmic Microwave Background (CMB) temperature. Deuterium is by far the most sensitive of the light elements to η , and thus the baryon density, and determining the primordial value of D/H (the deuterium to hydrogen abundance) has been the focus of intense research efforts over the last three decades (e.g. York & Rogerson 1976; Vidal-Madjar et al. 1977; Laurent, Vidal-Madjar & York 1979; Pettini & Bowen 2001; O’Meara et al. 2001; Hebrard et al. 2002; Moos et al. 2002; Sonneborn et al. 2002; Kirkman et al. 2003; Sembach

^{*} Based on observations made with ESO Telescopes at the Paranal Observatories under programme ID 076.C-0503(A)
[†] Email: sarae@uvic.ca

et al. 2004; Wood et al. 2004; Oliveira et al. 2006). These efforts have made a two-pronged attack, by measuring D/H abundances both in the Milky Way and at high redshifts. Although D is not produced in any significant quantities after Big Bang nucleosynthesis, it is easily astrated in stars, so measurements at high redshifts could potentially yield the primordial abundance more readily than observations in the local universe. High redshift measurements can be achieved with observations of high HI column density absorption systems in the lines of sight towards QSOs, such as the damped Lyman alpha systems (DLAs) and Lyman limit systems (LLSs). However, since the DI Lyman α line is only separated from that of HI by ~ 80 km/s, only those rare absorbers with very simple velocity structure yield reliable results. Thus, despite a decade of high redshift work, only six robust measurements of D/H at high redshift currently exist (O’Meara et al. 2001; Pettini & Bowen 2001; Kirkman et al. 2003; O’Meara et al. 2006). Nonetheless, these measurements paint a relatively coherent picture and yield an Ω_b (inferred from a mean $D/H = (2.8 \pm 0.4) \times 10^{-5}$)¹ that is in solid agreement (i.e. within the 1σ errors) with that determined from CMB experiments such as WMAP (see Pettini 2006 for a review).

Measurements of D/H in the Milky Way complement high redshift observations by providing an order of magnitude more sightlines in which abundances can be measured (see Linsky et al. 2006 for the most recent compilation). Although some astration has probably occurred, the highest Galactic D/H ratios set a lower limit to the primordial abundance. Moreover, modelling the amount of astration inferred from sub-primordial abundances provides clues to the rate at which material has been processed in stars – a vital ingredient in chemical evolution models. For these reasons, one of the principle drivers of the Far-Ultraviolet Spectroscopic Explorer (FUSE) was to compile a large database of Galactic D/H measurements: ‘The main science goal of the FUSE mission has been to obtain accurate measurements of $(D/H)_{\text{gas}}$ for many sightlines in the Milky Way Galaxy and beyond in order to measure $(D/H)_{\text{prim}}$ and to obtain constraints on Galactic chemical evolution’ (Linsky et al. 2006). However, despite a massive investment of telescope resources from both FUSE and other satellite facilities, and measurements of D/H in almost 50 lines of sight, the picture of Galactic deuterium abundances remains puzzling. On the one hand, inside the Local Bubble (< 100 pc from the Sun) the D/H value seems roughly constant at 1.5×10^{-5} , approximately 60% of the primordial value. However, beyond this bound, there is a large scatter in the D/H ratios which can not be easily explained by astration (Jenkins et al. 1999; Wood et al. 2004; Draine, 2006). As pointed out by Draine (2006), there is an observed factor of five range in D/H for clouds within 100 pc. It is difficult to reconcile such disparate abundances, on such small spatial scales, within a chemical evolution model, particularly since mixing should be efficient on these scales (e.g. Romano et al. 2006).

At the present time, the most favoured explanation for the variation in Galactic D/H ratios is the depletion of deu-

terium from the gas phase onto grains. Deuterium depletion was first suggested over 20 years ago by Jura (1982) and then explored theoretically by Tielens (1983). The most recent theoretical work has been done by Draine (2004, 2006) who suggested that deuterated polycyclic aromatic hydrocarbons (PAHs) in cold dust could be sufficient sinks for deuterium to explain the scatter in Galactic measurements. Empirical support for D depletion comes from the composition of interstellar grains collected in the upper terrestrial atmosphere which can be enriched by D relative to the usual meteoritic composition (Keller, Messenger & Bradley 2000). Whilst the quantity of deuterium was not sufficient to explain the Galactic ISM abundances, the presence of dust phase D does act as a ‘proof of concept’.

One empirical test of the depletion scenario is to look for correlations between D/H and the abundances of other refractory elements. This test was first done by Prochaska, Tripp & Howk (2005) using far-blue optical lines of Ti II measured in Keck/HIRES spectra for seven Galactic sightlines. Prochaska et al. (2005) noted a possible correlation at the 95% level, although this was strongly driven by a single high D/H sightline. Moreover, Prochaska et al. note that the literature limit for a second high D/H sightline (γ^2 Vel) does not agree with the overall trend in their data and that there is a large scatter in Ti/H at low D/H. More recently, Linsky et al. (2006) have presented corroborating evidence for depletion correlations based on Si and Fe; both elements show significant abundance trends with D/H. Linsky et al. also tentatively suggest that a possible correlation between D/H and the gas temperature derived from H_2 may also support the dust scenario. Savage et al. (2007) have also supported the dust depletion model, since their high value (2.2×10^{-5}) of D/H in the warm neutral medium of the Galactic halo is consistent with expulsion of material from the disk and associated ablation of dust particles.

In this paper, we extend previous analyses of refractory elements by significantly enlarging the sample of Ti measurements in the local ISM. Due to its highly refractory nature (e.g. Savage & Sembach 1996; Jenkins 2004), Ti should provide one of the most sensitive measurements of depletion and therefore correlate most steeply with D/H. A further advantage of Ti II is its ionization potential (IP) of 13.6 eV which means that ionization corrections will be less than for other commonly detected species such as Fe II (IP=16.2 eV) and Si II (IP=16.3 eV).

2 OBSERVATIONS AND DATA ANALYSIS

We chose targets with measured D/H and whose $\log N(\text{HI}) > 19.7$. This criterion ensures that Ti II lines will have detectable equivalent widths (EWs) and that ionization corrections will be a negligible concern.

2.1 Observations and Data Reduction

Our final sample of Ti II lines in the local Galactic disk comprises data obtained from the following sources: the pilot survey of Prochaska et al. (2005) (7 stars), VLT/UVES data obtained from the archive (2 stars), VLT/UVES data

¹ The error on the D/H abundance from QSO absorption lines is estimated from a jackknife analysis of the weighted means of six robust measurements.

Table 1. Journal of Observations

| Star | Mag (V) | RA (J2000) | Dec (J2000) | Distance (pc) | Instrument | Run |
|----------------|---------|------------|--------------|-------------------------------------|------------|----------------|
| δ Ori | 2.23 | 05 32 00.4 | −00 17 57 | 281±65 | HIRES | September 2004 |
| ι Ori | 2.77 | 05 35 26.0 | −05 54 35.6 | 407±127 | HIRES | September 2004 |
| ϵ Ori | 1.70 | 05 36 12.8 | −01 12 06.9 | 412±154 | HIRES | September 2004 |
| μ Col | 5.17 | 05 45 59.9 | −32 18 23.2 | 400 ⁺¹⁰⁰ _{−70} | UVES | Archive |
| HD 41161 | 6.76 | 06 05 52.5 | +48 14 57.4 | 1253 | HIRES | April 5 2006 |
| HD 53975 | 6.47 | 07 06 36.0 | −12 23 38.2 | 1318 | HIRES | April 5 2006 |
| ζ Pup | 2.25 | 08 03 35.1 | −40 00 11.3 | 429±94 | UVES | Period 76 |
| γ^2 Vel | 1.78 | 08 09 32.0 | −47 20 11.7 | 258±35 | UVES | Period 76 |
| WD 1034+001 | 13.22 | 10 37 04.0 | −00 08 20 | 155 ⁺⁵⁸ _{−48} | HIRES | June 2006 |
| θ Car | 2.76 | 10 42 57.4 | −64 23 40.0 | 135±9 | UVES | Period 76 |
| α Cru | 1.33 | 12 26 35.9 | −63 05 56.7 | 98±6 | UVES | Period 76 |
| β Cen | 0.61 | 14 03 49.4 | −60 22 22.9 | 161±16 | UVES | Archive |
| BD+39°3226 | 10.18 | 17 46 31.9 | +39 19 09.07 | 290 ⁺¹⁴⁰ _{−70} | HIRES | April 5 2006 |
| HD 191877 | 6.26 | 20 11 21.0 | +21 52 29.8 | 2200±550 | HIRES | September 2004 |
| HD 195965 | 6.98 | 20 32 25.6 | +48 12 59.3 | 794±200 | HIRES | September 2004 |
| HD 206773 | 6.9 | 21 42 24.2 | +57 44 10 | 500 ⁺²⁰⁰ _{−120} | HIRES | June 2006 |
| BD+28°4211 | 10.51 | 21 51 11.0 | +28 51 50.4 | 104±18 | HIRES | October 2004 |
| HD 209339 | 6.69 | 22 00 39.3 | +62 29 16.0 | 850 | HIRES | June 2006 |
| Feige 110 | 11.83 | 23 19 58.4 | −05 09 56.2 | 179 ⁺²⁶⁵ _{−67} | HIRES | September 2004 |

obtained through a Period 76 ESO allocation (4 stars) and new HIRES observations obtained in 2006 (6 stars). For completeness, we list all targets from our Ti II survey (which include those already published in Prochaska et al. 2005) in Table 1, but only describe the data acquisition of previously unpublished data in the following sections. The distances to the stars are taken from the compilation of Linsky et al. (2006), supplemented by values from Pan et al. (2004), Oliveira & Hebrard (2006) and Hebrard et al. (2005a).

2.1.1 HIRES Data

The new HIRES data were obtained, primarily during twilight, on the nights of 06 April 2006, 02 June 2006, 03 June 2006, and 25 December 2006. All of the data were acquired with the 0.4'' wide, E3 decker which affords a FWHM resolution of $\approx 3\text{km s}^{-1}$. We reduced these data using the HIREDUX pipeline (v. 2.1; Bernstein et al., in preparation) developed using the IDL software package and distributed within the XIDL package (<http://www.ucolick.org/~xavier/IDL/index.html>). In brief, the pipeline bias subtracts and flatfields each science and calibration image. It traces the order curvature across each chip (limited to the blue CCD for these observations) and derives a 2D wavelength solution from the ThAr images.

For these very bright targets, the biggest background is scattered light. This component is fit with a 2D surface by measuring the signal between echelle orders. The fit is interpolated across the orders and subtracted from the image. The RMS error in this signal is typically less than 5 electrons. We then boxcar extracted the stars (the S/N is too large for optimal extraction to be advantageous) to derive a 1D spectrum and co-added the individual exposures, weighting by the median S/N.

2.1.2 Archival UVES Data

Data for μ Col and β Cen were downloaded from the ESO archive. A considerable amount of data were available but we selected a subset whose settings offered the highest resolution and maximum exposure times at the wavelengths of interest. For β Cen we used only 1x1 binned data with 4 central wavelengths: 346 nm (slit width = 0.5 arcsec), 390 nm (slit width = 0.44 arcsec), 437 nm (slit width = 0.5 arcsec) and 564 nm (slit width = 0.3 arcsec) yielding a FWHM resolution ranging from $R \sim 70,000$ to 90,000 depending on the slit and the CCD. For μ Col, the data were more limited and often had sub-optimal instrument set-ups (such as very wide slits). We therefore used only 1 central wavelength setting, 390 nm, with 2x2 binning and a 1 arcsec slit yielding a FWHM resolution $R \sim 45,000$. Although a set of MIDAS scripts exists to form a UVES pipeline, we found that the pipeline reduction had considerable trouble dealing with very high S/N data (a well-known problem). For consistency, we therefore decided to apply the HIREDUX IDL reduction pipeline to the UVES data. This process worked well in general, although the final extracted spectra had considerable structure in the continuum (perhaps owing to poor flat-fielding), particularly in the blue orders. We attempted to fit out this structure during the continuum fitting process. This process was judged to be quite successful, based on the consistency of EWs of a given interstellar species between different orders, settings and transitions (see next section).

2.1.3 UVES Period 76 Data

For 4 southern stars not available in the archive, we received an ESO allocation in Period 76 (October 2005 – March 2006). In all cases we used the same combination of settings: 1x1 binning, 0.5 arcsec slit and 3 central wavelengths, 346 nm, 390 nm and 580 nm yielding a typical resolution $R \sim 80,000$. As for the archival UVES data, we used the adapted version of the HIRES IDL pipeline and fitted out

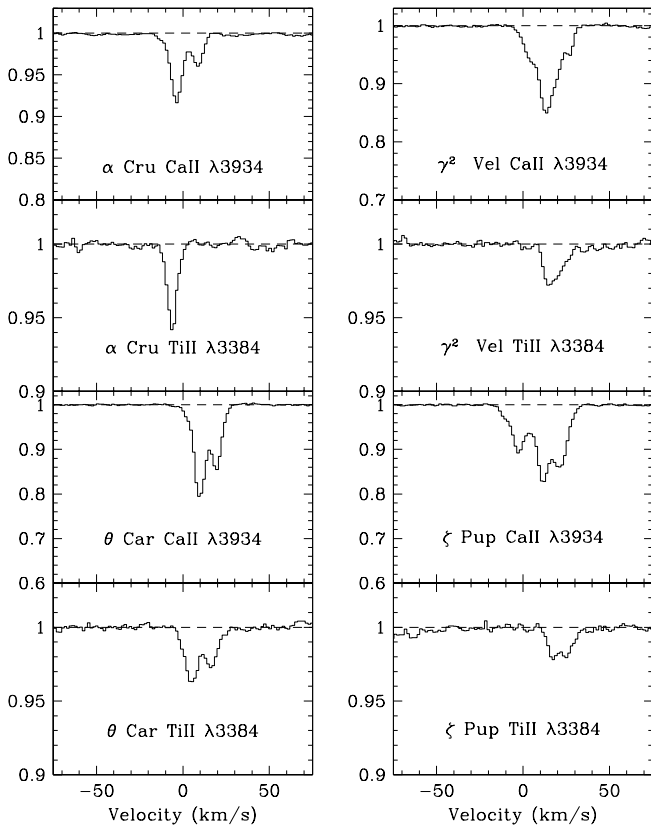


Figure 1. Normalized sections of spectra around the transitions of Ti II λ 3384 and Ca II λ 3934 for 4 of our program stars (see also Figure 2 and 3). Note the different y-axes from panel to panel.

the structure in the blue orders along with the underlying continuum.

3 RESULTS

3.1 Analysis

To determine gas phase column densities we use the VPFIT² software to decompose the absorption into individual components. The total column density is then calculated from the sum of these components. Profiles of Ti II λ 3384, plus Ca II λ 3934 are shown in Figures 1, 2 and 3. In many lines of sight, Ti II λ 3242 is also detected, in which case we simultaneously fit the two transitions. The very small EWs (typically 10-20 mÅ) of the Ti II lines coupled with the b -values (which indicate that the lines are resolved) show that it is unlikely that saturation affects these transitions. This is confirmed by an optical depth analysis of the two Ti II lines which yields consistent results for both. In the UVES data and a small subset of the HIRES data, Ca II λ 3969 is also covered so that, when detected, it is simultaneously fit with Ca II λ 3934. In the case of WD1034+001, the Ti II and

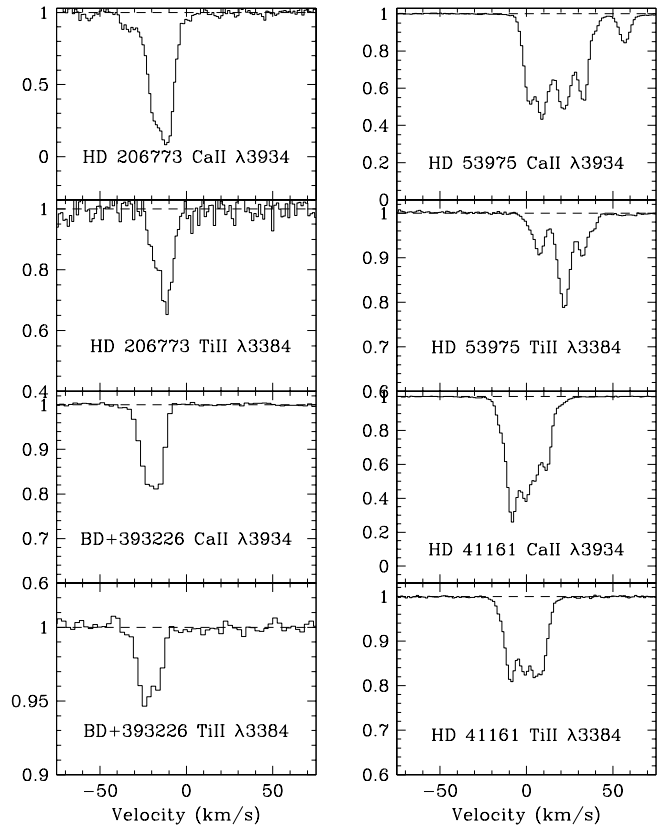


Figure 2. Normalized sections of spectra around the transitions of Ti II λ 3384 and Ca II λ 3934 for 4 of our program stars (see also Figures 1 and 3). Note the different y-axes from panel to panel.

Ca II lines are barely detected, so the fit is very uncertain. In this case, we therefore additionally estimate the column density from the apparent optical depth of the absorption lines. For μ Col, the Ti II λ 3384 line is detected at $< 3\sigma$ significance, so we quote a limit. We determine the errors on the lines in two different ways. First, we consider the formal error on the total column density returned by VPFIT³. Next, we separately fit the different transitions of the same species, as well as fitting lines of a given species that are covered by multiple orders, or multiple settings. This is particularly useful for the assessment of systematic errors such as the continuum fit, a particular concern for the blue UVES data. However, we found that the separate fits exhibited excellent agreement, usually within 0.02 dex. Due to the very high S/N of the spectra, the range of column densities determined from individual line fits usually dominated the formal error from VPFIT, so that the former was adopted as the final quoted uncertainty in Table 2. We exclude two of the sightlines from our analysis of depletion patterns. First, HD 206773 has poorly determined D/H due to severe saturation of the D I lines (Hebrard et al. 2005a). Second, although

² <http://www.ast.cam.ac.uk/~rfc/vpfit.html>

³ The errors on individual component column densities are also returned, but these are considerably more unreliable.

Table 2. Column Density Data

| Star | N(H) | N(D) | N(OI) | N(TiII) | N(CaII) | N(FeII) | N(SiII) | Refs |
|-------------------------------|--------------------------|--------------------------|--------------------------|------------------|------------------|--------------------------|--------------------------|--------------|
| δ Ori | 20.19 \pm 0.03 | 15.06 \pm 0.12 | 16.67 \pm 0.05 | 11.15 \pm 0.04 | ... | 14.08 \pm 0.03 | ... | 1, 2, 3, 4 |
| ι Ori | 20.18 $^{+0.06}_{-0.07}$ | 15.30 $^{+0.04}_{-0.05}$ | 16.76 \pm 0.09 | 11.31 \pm 0.03 | ... | 14.20 $^{+0.20}_{-0.15}$ | 15.16 $^{+0.02}_{-0.03}$ | 1, 3, 4, 5 |
| ϵ Ori | 20.45 \pm 0.08 | 15.25 \pm 0.05 | 16.98 \pm 0.05 | 11.40 \pm 0.03 | ... | 14.20 \pm 0.10 | 15.02 $^{+0.08}_{-0.12}$ | 1, 3, 4, 5 |
| μ Col | 19.86 \pm 0.02 | 14.7 $^{+0.3}_{-0.1}$ | ... | <11.4 | 12.13 \pm 0.02 | 14.13 \pm 0.02 | 15.10 \pm 0.02 | 4, 6 |
| HD 41161 | 21.08 \pm 0.09 | 16.41 \pm 0.05 | 18.04 \pm 0.05 | 12.28 \pm 0.04 | 12.54 \pm 0.01 | 14.98 \pm 0.06 | ... | 7 |
| HD 53975 | 21.14 \pm 0.06 | 16.15 \pm 0.07 | 17.87 \pm 0.08 | 12.13 \pm 0.04 | 12.56 \pm 0.01 | 14.84 \pm 0.05 | ... | 7 |
| ζ Pup | 19.96 \pm 0.03 | 15.11 \pm 0.06 | ... | 11.07 \pm 0.04 | 11.83 \pm 0.02 | 14.13 $^{+0.17}_{-0.07}$ | 15.07 $^{+0.07}_{-0.02}$ | 4, 8 |
| γ^2 Vel | 19.71 \pm 0.03 | 15.05 \pm 0.03 | ... | 11.10 \pm 0.02 | 11.61 \pm 0.02 | 13.95 \pm 0.11 | 15.03 \pm 0.04 | 4, 8 |
| WD 1034+001 | 20.07 \pm 0.07 | 15.40 \pm 0.07 | 16.60 \pm 0.10 | 11.1 \pm 0.2 | 11.35 \pm 0.15 | 14.10 \pm 0.10 | ... | 4, 9 |
| θ Car | 20.28 \pm 0.10 | 14.98 $^{+0.18}_{-0.21}$ | 16.42 \pm 0.20 | 11.31 \pm 0.01 | 11.65 \pm 0.01 | 14.19 \pm 0.03 | 14.38 $^{+0.25}_{-0.08}$ | 4, 10 |
| α Cru | 19.85 \pm 0.10 | 14.95 \pm 0.05 | ... | 11.12 \pm 0.02 | 11.23 \pm 0.05 | 14.00 \pm 0.10 | ... | 4, 6 |
| β Cen | 19.63 \pm 0.10 | 14.7 \pm 0.2 | ... | 11.05 \pm 0.04 | 11.12 \pm 0.04 | 13.92 $^{+0.05}_{-0.04}$ | 14.59 \pm 0.01 | 4, 6, 11 |
| BD+39 $^{\circ}$ 3226 | 20.08 \pm 0.09 | 15.15 \pm 0.05 | 16.40 \pm 0.10 | 11.49 \pm 0.08 | 11.67 \pm 0.01 | 14.15 \pm 0.07 | 14.80 \pm 0.20 | 4, 9 |
| HD 191877 | 21.10 \pm 0.07 | 15.95 $^{+0.11}_{-0.06}$ | 17.54 $^{+0.20}_{-0.12}$ | 12.24 \pm 0.02 | ... | 14.95 \pm 0.02 | ... | 3, 4, 12, 13 |
| HD 195965 | 21.01 \pm 0.05 | 15.89 \pm 0.07 | 17.77 $^{+0.04}_{-0.06}$ | 12.02 \pm 0.02 | ... | 14.81 \pm 0.01 | ... | 3, 4, 12, 13 |
| HD 206773 † | 21.10 \pm 0.05 | 17.0 \pm 0.5 | 17.85 \pm 0.05 | 12.16 \pm 0.02 | 12.65 \pm 0.02 | ... | ... | 14 |
| BD +28 $^{\circ}$ 4211 | 19.85 \pm 0.02 | 14.99 \pm 0.03 | 16.22 \pm 0.10 | 11.08 \pm 0.08 | ... | 14.10 \pm 0.10 | ... | 3, 4, 15 |
| HD 209339 †† | \sim 21.5 | ... | ... | 12.14 \pm 0.03 | 12.68 \pm 0.03 | ... | ... | 16 |
| Feige 110 | 20.14 \pm 0.07 | 15.47 \pm 0.06 | 17.06 \pm 0.15 | 11.59 \pm 0.03 | ... | ... | ... | 3, 17, 18 |

Upper limits are 3σ . † Included here for completeness, but not used in analysis due to saturation of DI lines (Hebrard et al. 2005a). †† Included here for completeness, FUSE deuterium data still under analysis (C. Oliveira, private communication). Refs: 1 - Meyer et al. (1998); 2 - Jenkins et al. (1999); 3 - Prochaska et al. (2005); 4 - Linsky et al. (2006); 5 - Laurent et al. (1979); 6 - York & Rogerson (1976); 7 - Oliveira & Hebrard (2006); 8 - Sonneborn et al (2000); 9 - Oliveira et al. (2006); 10 - Allen et al (1992); 11 - van Steenberg & Shull (1988); 12 - Hoopes et al. (2003); 13 - Liszt (2006); 14 - Hebrard et al. (2005a); 15 - Sonneborn et al. (2002); 16 - C. Oliveira, private communication; 17 - Friedman et al. (2002); 18 - Hebrard et al. (2005b)

HD 209339 has FUSE data which will eventually permit an analysis of the D/H in this sightline, the data have not yet been analysed. We tabulate the column densities of Ti II and Ca II for completeness, but do not consider these sightlines further in our analysis.

For metal line species, we quote in Table 2 the column densities of the single atomic or ionic species that is measured in our (or literature) data. However, Liszt (2006) has shown that the molecular contribution to D and H can be important and that ignoring its contribution can lead to an over-estimate of the D/H ratio (see also Lacour et al. 2005). We therefore use total column densities for hydrogen and deuterium, accounting for both molecular and atomic gas, i.e. $N(\text{H})=N(\text{HI})+2N(\text{H}_2)+N(\text{HD})$ and $N(\text{D})=N(\text{DI})+N(\text{HD})$. For most sightlines, the molecular contribution is orders of magnitude less than the atomic column density such that $N(\text{H}) \sim N(\text{H I})$ and $N(\text{D}) \sim N(\text{D I})$. However, a significant effect is present for HD 41161, HD 53975, HD 191877, HD 195965, HD 206773 and HD 209339 (although these latter two are not used in our main analysis). The largest effect is seen towards HD 41161 where D I/H I = 25.1 parts per million (ppm) and D/H = 21.4 ppm (Oliveira & Hebrard 2006), a difference of $\sim 15\%$.

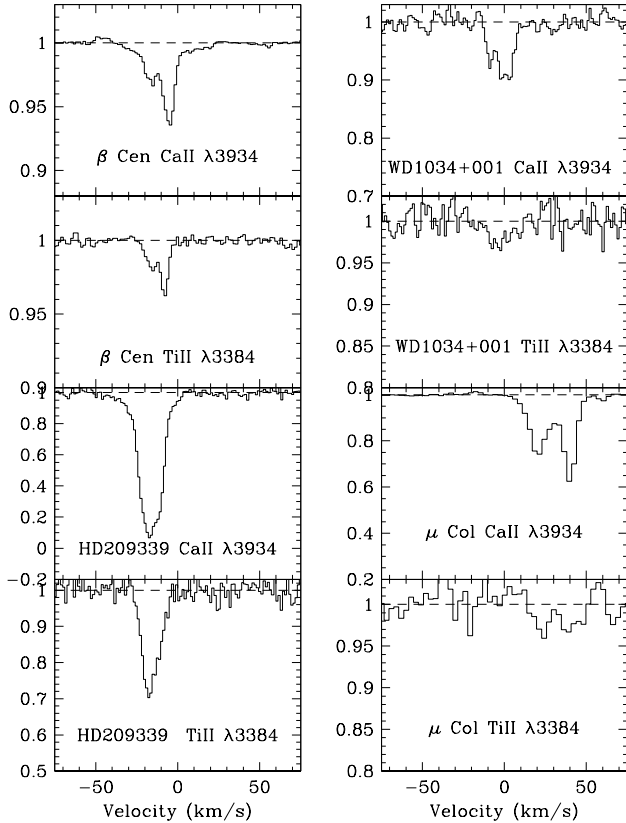
3.2 Correlations with D/H

In Figure 4 we present the first main result of this analysis. The abundance of Ti, on both linear (in units of parts per billion, ppb) and logarithmic (relative to solar) scales is plotted versus D/H in units of ppm. For logarithmic abundances, we use the standard notation $[X/\text{H}] = \log (X/\text{H})$

$-\log (X/\text{H})_{\odot}$, which is analogous to the notation $D(X)$ used by Linsky et al. (2006). For solar abundances, we use the compilation of Lodders (2003), except for oxygen, for which we adopt the value from Holweger (2001) where a full non-LTE treatment was adopted. These values are $\log [N(X)_{\odot}/N(\text{H})_{\odot}] = -4.46, -4.53, -7.08, -3.26$ for Si, Fe, Ti and O respectively. For convenience, in Table 3 we show the relative abundances used for Figures 4 and 5. We include data from Prochaska et al. (2005) and perform a least-squares fit of the form $y = mx + c$ to the final Ti sample which consists of 16 detections. The best fit straight line for $[\text{Ti}/\text{H}]$ has values $m = 0.016 \pm 0.007$ and $c = -1.95 \pm 0.09$ where errors were determined by randomly re-generating the $[\text{Ti}/\text{H}]$ vs. D/H distribution 1000 times based on the quoted 1σ errors. Spearman's rank correlation statistic is 0.55, yielding a rejection of the null hypothesis (that there is no correlation) at the 97% level. In addition to the enlargement of the sample size, one of the important contributions of this work is the inclusion of 3 new high D/H data points, as well as the lowest D/H in the current sample. The correlation of Prochaska et al. (2005) was pivotal upon a single high datum (Feige 110); removal of this one point reduces the significance of the correlation from 95% to 86%. Moreover, for one other high D/H sightline in the literature, Prochaska et al. (2005) pointed out that the upper limit for γ^2 Vel (D/H=21.9 ppm) of $[\text{Ti}/\text{H}] \leq -1.82$ reported by Welsh et al. (1997) was potentially inconsistent with the depletion trend. With a larger sample, and more high D/H points, we can now make a more robust assessment of the D/H correlation. First, we find that with higher S/N data, the measured value of $[\text{Ti}/\text{H}] = -1.53$ for γ^2 Vel is in actually excellent agreement with the high D/H point (Feige 110) presented in Prochaska

Table 3. Abundances

| Star | (D/H) _{ppm} | [Ti/H] | [Si/H] | [Fe/H] | log < n(H) > |
|----------------|----------------------|------------------|------------------|------------------|------------------|
| δ Ori | $7.4^{+2.4}_{-1.8}$ | -1.96 ± 0.05 | ... | -1.58 ± 0.04 | -0.75 ± 0.04 |
| ι Ori | $13.2^{+2.6}_{-2.2}$ | -1.76 ± 0.07 | -0.53 ± 0.06 | -1.42 ± 0.18 | -0.95 ± 0.04 |
| ϵ Ori | $6.3^{+1.5}_{-1.2}$ | -1.97 ± 0.09 | -0.97 ± 0.13 | -1.72 ± 0.13 | -0.65 ± 0.08 |
| μ Col | $6.9^{+4.1}_{-2.6}$ | < -1.38 | -0.30 ± 0.03 | -1.20 ± 0.03 | -1.23 ± 0.01 |
| HD 41161 | $21.4^{+5.7}_{-4.5}$ | -1.72 ± 0.10 | ... | -1.57 ± 0.11 | -0.51 ± 0.08 |
| HD 53975 | $10.2^{+2.4}_{-2.0}$ | -1.93 ± 0.07 | ... | -1.77 ± 0.08 | -0.47 ± 0.09 |
| ζ Pup | $14.1^{+2.0}_{-2.4}$ | -1.81 ± 0.05 | -0.43 ± 0.06 | -1.30 ± 0.10 | -1.16 ± 0.02 |
| γ^2 Vel | $21.9^{+2.2}_{-2.0}$ | -1.53 ± 0.05 | -0.22 ± 0.05 | -1.23 ± 0.11 | -1.19 ± 0.01 |
| WD 1034+001 | $21.4^{+5.5}_{-4.4}$ | -1.89 ± 0.21 | ... | -1.44 ± 0.12 | -0.61 ± 0.08 |
| θ Car | $5.0^{+3.4}_{-2.0}$ | -1.89 ± 0.10 | -1.44 ± 0.22 | -1.56 ± 0.10 | -0.34 ± 0.03 |
| α Cru | $12.6^{+3.7}_{-2.9}$ | -1.65 ± 0.10 | ... | -1.32 ± 0.14 | -0.63 ± 0.01 |
| β Cen | $11.7^{+7.9}_{-4.7}$ | -1.50 ± 0.11 | -0.58 ± 0.10 | -1.18 ± 0.11 | -1.07 ± 0.01 |
| BD+39° 3226 | $11.7^{+3.1}_{-2.5}$ | -1.51 ± 0.12 | -0.82 ± 0.22 | -1.40 ± 0.11 | -0.87 ± 0.05 |
| HD 191877 | $7.1^{+2.3}_{-1.7}$ | -1.78 ± 0.07 | ... | -1.62 ± 0.07 | -0.73 ± 0.05 |
| HD 195965 | $7.6^{+1.7}_{-1.4}$ | -1.91 ± 0.05 | ... | -1.67 ± 0.05 | -0.38 ± 0.11 |
| BD+28° 4211 | $13.8^{+1.2}_{-1.1}$ | -1.69 ± 0.08 | ... | -1.22 ± 0.10 | -0.66 ± 0.04 |
| Feige 110 | $21.4^{+5.1}_{-4.1}$ | -1.47 ± 0.08 | ... | ... | -0.60 ± 0.35 |

**Figure 3.** Normalized sections of spectra around the transitions of Ti II λ 3384 and Ca II λ 3934 for 4 of our program stars (see also Figure 1 and 2). Note the different y-axes from panel to panel.

et al. Moreover, the highest D/H sightline (HD41161) in our sample is also in good agreement with the general trend of increasing Ti/H with D/H. However, the third high D/H sightline, WD1034+001 exhibits a low Ti/H for its D/H, although this point has the largest error bars on its measured N(Ti II) column density due to the low significance of the detection (see Figure 3 and Tables 2 and 3).

Given the discrepancy noted above between the literature upper limit and our measured value for [Ti/H] towards γ^2 Vel, it is interesting to compare other sightlines for which literature values also exist. Welsh et al. (1997) report a limit on the column density of Ti II towards θ Car that is half of our measured value and the discrepancy towards ζ Pup is even higher: 0.45 dex, almost a factor of three. However, the Ca II abundances in the sightlines common to this work and Welsh et al. (1997) are in good agreement within the errors, with differences ≤ 0.08 dex. Hunter et al. (2006) have also previously noted consistency in N(Ca II) and discrepancies in N(Ti II) between high S/N UVES data and previous works, whose S/N ratios are typically < 50 . Hunter et al. attributed this to the weakness of the Ti II lines, relative to Ca II. Confirmation of this effect here highlights the importance of very high S/N ratios and spectral resolution to make these measurements accurately.

4 DISCUSSION

4.1 Dust Depletion

Previous authors have interpreted the correlation between the gas-phase abundance of refractory elements and (D/H) as evidence that differential depletion leads to low values for each (Prochaska et al. 2005; Linsky et al. 2006). Although the trend traced by our enlarged sample of Ti/H values supports this interpretation qualitatively, a closer examination of the results leads to a less clear cut picture. Focus first on the abundance trends from different elements. In Figure 4 we overlay the fits for depletion of Fe and Si from Linsky et al. (2006) with our own Ti results. If dust depletion is

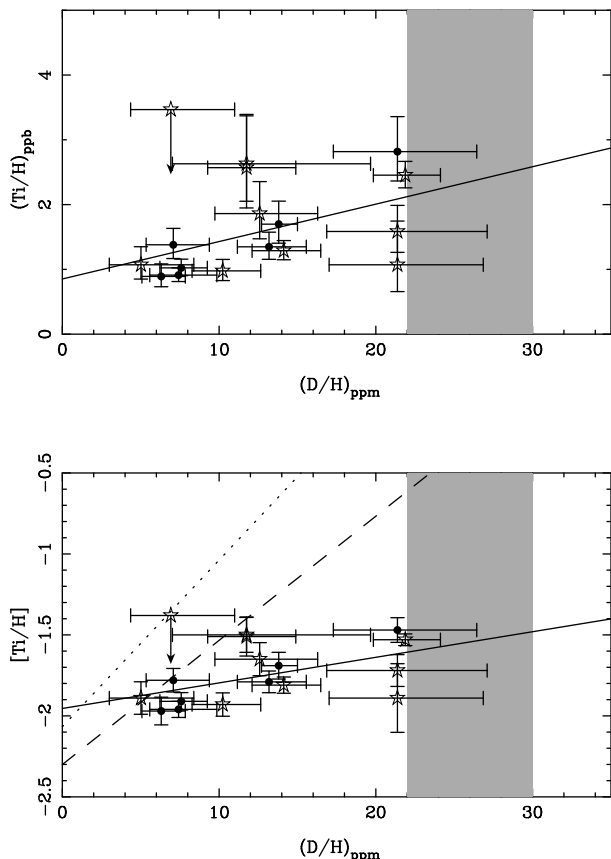


Figure 4. Ti abundance as a function of D/H. Results from this work are shown by stars; filled circles are data points taken from Prochaska et al. (2005). The solid line shows the least squares best fit to all 16 detections. The shaded region shows the constraints on the primordial value of D/H determined from quasar absorption line systems. In the top panel, we show linear-linear axes for Ti/H (in parts per billion, ppb) and D/H (in parts per million, ppm), the best fit line $y = mx + c$ has $m = 0.06 \pm 0.03$ and $c = 0.85 \pm 0.32$. In the lower panel, we use a logarithmic y-axis to facilitate comparison with other elements, the best fit line $y = mx + c$ has $m = 0.016 \pm 0.006$ and $c = -1.95 \pm 0.08$. The fits to Fe and Si abundances from Linsky et al. (2006) are shown with dashed and dotted lines respectively.

the cause of the correlation of abundance with D/H then we expect a steeper gradient for more refractory elements. In the case of Ti, Fe and Si, the former is the most refractory and the latter the least sensitive to depletion (e.g. Savage & Sembach 1996). The relative gradients in Figure 4 are therefore inconsistent with our simple predictions from a ‘standard’ depletion scenario, since we would expect Ti to be considerably steeper than Fe or Si. Indeed, the gradient seen in Ti is only marginally steeper than that found for [O/H] which is only very mildly refractory. Therefore, although the existence of trends between refractory elements and D/H support a picture of dust depletion, quantitatively the gradients are inconsistent with this scenario. Steigman, Romano & Tosi (2007) have also questioned the dust depletion scenario due to their failure to find a trend between line of sight reddening and D/H, as one might have expected were dust the cause of lower D/H values.

In section 3.1 we argued that saturation of the Ti II

lines is unlikely to be a serious concern. However, some of the Fe II and Si II transitions have considerably higher optical depths (e.g., Redfield & Linsky 2002). There is an anti-correlation between [Fe/H] and N(Fe II) in the compilation of Linsky et al. (2006). If saturation systematically underestimates N(Fe II) for the low [Fe/H] data points, the true slope of the correlation with D/H will be flatter than observed. However, this effect is unlikely to be large enough to yield a true gradient of [Fe/H] versus D/H that is flatter than the [Ti/H] versus D/H correlation. Moreover, there is a mild correlation between [Si/H] and N(Si II), so that any correction for saturation would make the dotted line in Figure 4 steeper, thus accentuating the difference with the [Ti/H] correlation. It is also possible that the D lines may suffer from saturation, and this may be particularly relevant for the high N(HI) lines of sight studied here. However, it is difficult to apply horizontal shifts to the D/H values in our sample that would make the correlation with [Ti/H] steeper. It therefore seems unlikely that saturation effects can explain the relative slopes in Figure 4.

We can further investigate depletion trends by considering correlations with mean hydrogen densities. It is well known that depletion in the Galactic ISM correlates with $\langle n(H) \rangle$, the mean volume density of hydrogen (e.g. Savage & Bohlin 1979; Phillips, Gondhalekar & Pettini 1982; Spitzer 1985; Gondhalekar 1985; Jenkins et al. 2004) where

$$\langle n(H) \rangle = \frac{N(HI) + 2N(H_2)}{\text{distance}} \quad (1)$$

We calculate $\langle n(H) \rangle$ for the 17 sight lines in our Ti II sample and supplement them with five more sight lines in Linsky et al. (2006) which have H₂ measurements (Lan 23, TD1 32709, PG0038+199, LSS 1274, and HD 90087) see Table 3 and Figure 5. Jenkins (2004) parametrized ISM abundances in terms of a depletion factor, F_* , which in turn correlates with $\langle n(H) \rangle$. We performed a fit to the correlation between F_* and $\langle n(H) \rangle$ and using the parameters in Jenkins (2004), determined the corresponding relationship between $\langle n(H) \rangle$ and abundance for the 144 Galactic stars in his sample. For Ti, Si and Fe we determine:

$$[Ti/H] = -2.226(0.4 \langle n(H) \rangle + 0.8) - 0.844 - 0.01 \quad (2)$$

$$[Si/H] = -1.076(0.4 \langle n(H) \rangle + 0.8) - 0.223 \quad (3)$$

$$[Fe/H] = -1.198(0.4 \langle n(H) \rangle + 0.8) - 0.95 + 0.02 \quad (4)$$

The final term in the equations for [Ti/H] and [Fe/H] account for the slightly different solar abundance scale adopted by Jenkins (2004). This relationship between $\langle n(H) \rangle$ and ISM abundances is over-plotted with our data in Figure 5. The correlation between [Ti/H] and depletion factor in Jenkins (2004) is very steep (the steepest of the 15 elements he studies), and very tight (reduced $\chi^2 = 0.95$). The best least squares fit to our Ti data is shown by the dashed line in the top left panel of Figure 5. The slope is clearly much flatter than that reported Jenkins (2004) and flatter than both the least squares fits for Fe and Si. Moreover, the correlation between [Ti/H] and $\langle n(H) \rangle$ is not statistically significant: the Spearman rank correlation coefficient rules out the null hypothesis at $< 2\sigma$ (83%) significance. It is also interesting to note that the abundance of Si, which is the least depleted of the three elements discussed here, has the steepest gradient with $\langle n(H) \rangle$. This reflects the same, unexpected result

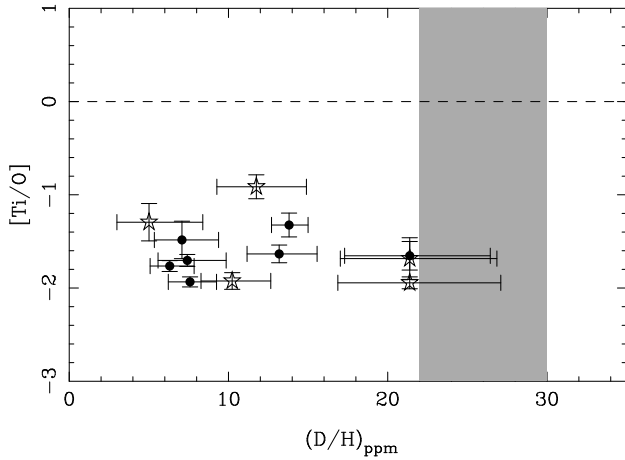


Figure 6. Relative Ti/O abundance as a function of D/H. Results from this work are shown by stars; filled circles are data points taken from Prochaska et al. (2005). The shaded region shows the constraints on the primordial value of D/H determined from quasar absorption line systems. For two elements with a similar nucleosynthetic origin, but different refractory properties, we expect a correlation with D/H if depletion onto dust is the cause of scatter in deuterium abundances.

presented in Figure 4, i.e. that the depletion fractions seem to be inverted relative to our expectations. This may indicate that the normal circumstances which govern the correlation between depletion and density in the ISM at large is not at work in these local (mostly $d < 500$ pc) sightlines. However, we should also stress that we have many fewer sightlines than the Jenkins sample, so that small number statistics could contribute to the absence of a tight correlation. Also noteworthy is the lack of correlation, and very large scatter at any given density, of $[D/H]^4$. We have only plotted in Figure 5 those stars in our Ti II sample. The same plot, but with a much larger sample extending to lower values of $\langle n(H) \rangle$, has been recently presented by Oliveira et al. (2006) who note that the scatter in D/H increases dramatically when $\langle n(H) \rangle > 0.1$, the regime in which most of our points lie. If lower D/H values do result from differential depletion, it appears from our Figure 5 that this depletion does not correlate with $\langle n(H) \rangle$. Oliveira et al. (2006) have attempted to fit an abundance/depletion model to their larger dataset and claim an anti-correlation between D/H and $\langle n(H) \rangle$. However, the reduced χ^2 for this fit is large (5.8), the scatter in D/H for a given $\langle n(H) \rangle$ is ~ 1 dex (similar to what is seen in our data) and the anti-correlation driven by just 2 data points. Indeed, some of the highest D/H values occur at the highest $\langle n(H) \rangle$. We therefore conclude that there is no convincing evidence for an anti-correlation between $\langle n(H) \rangle$ and D/H as one might expect from dust depletion.

Although the acceptance of dust depletion as the cause of the local variations of deuterium is gaining momentum, our results indicate that this interpretation is not clear cut. The same conclusion has also been recently reached by Steigman et al. (2007) who consider the evidence for dust

depletion as ‘ambiguous’. However, the above discussion assumes a very simple approach to the behaviour of dust in the local ISM. There are several caveats that should therefore be applied, such as the many flavours of dust that exist with different chemical compositions and the fact that dust production and destruction is likely to be a dynamic process. Moreover, current models of deuterium depletion involve D incorporation into deuterated PAHs (Draine 2004, 2006), different again from the grains which adsorb most refractory elements. Combined with the sightline averaged quantities that we are necessarily dealing with, some scatter in abundance relations is perhaps not surprising and we return to this issue in section 4.3. Shocks may also disrupt ‘normal’ depletion patterns. For example, weak shocks may be sufficient to release D from the dust phase (since deuterated PAHs are relatively fragile), whereas much stronger shocks may be required to ablate Ti grain material. These issues highlight the complexity of the ISM and abundance ratios and the caution that should be exercised in the interpretation that they are driven by dust.

4.2 Infall

An alternative scenario to the depletion of deuterium onto grains is the infall of unenriched gas from the halo which dilutes the abundance of chemical elements. Knauth, Meyer & Lauroesch (2006) have recently suggested local infall to explain the difference in N/O abundances at $d > 500$ pc, compared with closer sightlines. Romano et al. (2006) have also combined infall with astration to result in the relatively modest destruction ($f = (D/H)_{\text{prim}} / (D/H)_{\text{LISM}} \lesssim 1.8$) of deuterium from its primordial value. In most *simple* infall scenarios, the infalling gas has a D/H abundance that is close to the primordial value (i.e. higher than typical ISM values), whilst the abundances of other elements are lower than in the ambient disk ISM. This would result in an anti-correlation between heavy element abundance and D/H (e.g. Steigman et al. 2007), rather than the positive correlations depicted in Figure 4. Infall of low metallicity material could only explain the positive correlations seen in Figure 4 if the infalling low metallicity gas is also poor in deuterium. Although unlikely, we briefly explore this possibility here.

One might discriminate between the two scenarios of dust depletion versus various infall scenarios by examining relative abundances of different heavy elements. If infall of unenriched (or low metallicity, but with a solar abundance pattern) gas is responsible for the spatial variations in D/H, the relative abundances of two elements with similar nucleosynthetic origins should not correlate with D/H. Conversely, if the same two elements have different refractory properties, they should vary with D/H if depletion is the cause of variations in the deuterium abundance. In Figure 6 we compare the abundances of Ti and O, which are both α elements whose enrichment comes mainly through Type II supernovae of massive stars. Applying the above logic, one would expect a flat distribution of Ti/O vs. D/H in the infall scenario, but a positive correlation with D/H for dust depletion. The Spearman rank correlation coefficient is -0.1 , which indicates that there is no significant correlation between Ti/O and D/H, and the negative value actually indicates the data tend to an anti-correlation. Unfortunately, this test is not conclusive, since the very mild dependence

⁴ Here, $[D/H]$ represents the abundance relative to the primordial value, which we take to be 26 ppm.

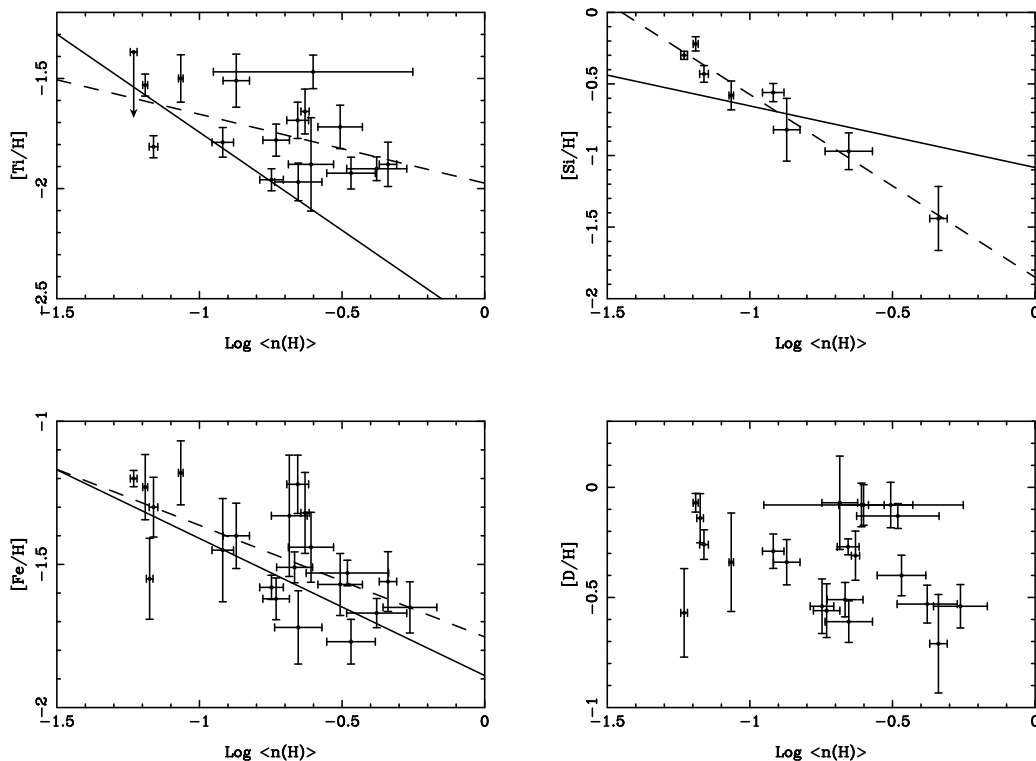


Figure 5. Abundances versus total hydrogen volume density, $n(\text{H})$ for a sample of local Galactic sightlines from Linsky et al. (2006) and this paper. Whereas Ti, Si and Fe are plotted relative to solar, the deuterium abundances are plotted relative to the primordial value, which we take to be 26 ppm. The solid lines show a fit to $[X/\text{H}]$ vs. $\langle n(\text{H}) \rangle$ determined from 144 stellar sightlines (Jenkins 2004). The dashed lines are the least squares fits to the data presented and have equations: $[\text{Ti}/\text{H}] = -0.31 \langle n(\text{H}) \rangle - 1.98$, $[\text{Si}/\text{H}] = -1.28 \langle n(\text{H}) \rangle - 1.86$, $[\text{Fe}/\text{H}] = -0.39 \langle n(\text{H}) \rangle - 1.75$.

of Ti/H on D/H (Figure 4) spans a factor of three less (0.5 dex) than the scatter in the Ti/O ratios at a given D/H .

We have already argued that a ‘standard’ infall scenario with low metallicity, enhanced D/H gas would cause an anti-correlation between $[X/\text{H}]$ and D/H . Although D-poor infall could qualitatively explain the positive correlations in Figure 4, again the gradients provide strong evidence against this possibility. If infalling gas has a low metallicity, but a solar abundance pattern, then in a plot of $[X/\text{H}]$ vs. D/H , every element should have the same gradient (ignoring all other effects such as depletion, ionization etc.). This is simply due to the fact that each element is diluted by the same amount and with a logarithmic ordinate, the Δy is a measure of the dilution factor. The very different slopes seen in Figure 4 therefore argue against a D-poor infall model, although we can not rule out more contrived models with highly non-solar abundances. However, combined with other evidence against the infall model, such as the relative constancy of certain elements such as O and Kr (Oliveira et al. 2005; Cartledge et al. 2004) and the sharp transition from approximately constant D/H inside the local bubble to a large scatter at distances beyond 100 pc, which would require a coincidentally very localized region of infall (e.g. de Avillez & Mac Low 2002), we conclude that infall is unlikely to be the main cause of local D/H variations. This is not to say that the local ISM is a closed box, in fact Romano et al. (2006) require some infall to explain the modest astration between the primordial D abundance and the local values.

4.3 Scatter

In closing this section, we note that for a given D/H , there is a wide range of observed $[\text{Ti}/\text{H}]$ abundances, spanning up to a factor of three (Figure 4). The scatter means that some $\text{D}/\text{H} \sim 10$ ppm sightlines have $[\text{Ti}/\text{H}]$ as high as the highest D/H sightlines, and vice versa. Linsky et al. (2006) discussed a number of factors that might contribute scatter in the relationship between element depletion and D/H such as line saturation of DI transitions, ionization corrections and $N(\text{HI})$ determination. The former of these may affect our results, although when saturation is obvious, we remove the sight line from our analysis (e.g. HD 206773). However, we expect the latter two concerns to be alleviated by our choice of high $N(\text{HI})$ sight lines. The more obvious damping wings should facilitate the determination of $N(\text{HI})$ that can be more challenging for $\log N(\text{HI}) < 19$ and the gas will be approaching complete self-shielding at these high column densities. In short, the observed scatter in Ti/H is most likely to represent true variations in the gas-phase abundance, not systematic effects. Such intrinsic scatter may be expected due to the dynamic nature of the ISM as dust is formed and ablated and the gas phase responds to photoionization and even incorporation into molecules. Steigman et al. (2007) have also argued that some amount of infalling gas that is not well mixed can not be ruled out. This will also contribute to intrinsic scatter in abundances.

5 CONCLUSIONS

We present 12 new measurements of Ti/H for local Galactic sightlines for which D/H measurements exist, almost tripling the sample from Prochaska et al. (2005). We investigate elemental abundance trends in the context of depletion of D onto grains as the cause for the large variation seen in D/H in the local Galactic disk (e.g. Wood et al. 2004 and references therein). Our data support the tentative correlation between Ti/H and D/H found by Prochaska et al. (2005), showing a correlation at 97% significance. However, it is not clear that this correlation can be explained by a simple depletion model. This conclusion is based on 1) the much shallower dependence of Ti/H on D/H than Si or Fe, despite the fact that the former is much more refractory and 2) the lack of a steep correlation between [Ti/H] and $\langle n(\text{H}) \rangle$. If the variation in Ti abundances of our sample sightlines were dominated by varying dust depletion, we would expect a very steep correlation with $\langle n(\text{H}) \rangle$, as has been previously found (Gondhalekar 1985; Jenkins 2004). Moreover, the correlation of Si/H versus D/H is steeper than between Fe/H and D/H, contrary to what is expected if these relations trace depletion, since Fe is more refractory than Si. This may mean that whatever effect is causing the flattening of the Ti depletion correlations that are normally seen in the ISM at large, may also affect Fe and Si, although probably to a lesser degree. However, the complex and dynamic nature of the ISM and dust depletion no doubt complicates the above simplistic expectations. Nonetheless, the shallow abundance correlations exhibited by titanium are somewhat surprising given previous ISM studies, and it is unclear why the depletion correlations have broken down in this sample. It may be due to superposition of the local bubble components whose physical environment could be quite different from the predominantly neutral disk ISM. However, only using stars at distances > 400 pc does not change our results and many stars in the Jenkins (2004) sample are at distances less than 500 pc. Finally, we have also argued that the gradients of [Si/H], [Fe/H] and [Ti/H] vs. D/H do not support a simple model of infall of metal-poor gas with solar abundances as the dominant cause of local D variations.

In summary, whilst the depletion of D onto grains remains a plausible explanation for the variation in D/H in the local ISM, our results show that this interpretation is far from clear cut.

ACKNOWLEDGMENTS

We are very grateful to Cristina Oliveira who provided detailed comments and expert advice on an earlier version of this manuscript and was generous in communicating results in advance of publication. We also benefitted from useful discussions and suggestions with Chris Howk, Ed Jenkins, Jeff Linsky, Max Pettini and Blair Savage. SLE is supported by an NSERC discovery grant and SL was partly supported by the Chilean *Centro de Astrofísica* FONDAF No. 15010003, and by FONDECYT grant N°1060823. Some of the data presented herein were obtained at the W.M. Keck Observatory, which is operated as a scientific partnership among the California Institute of Technology, the University of California and the National Aeronautics and Space Administration.

The Observatory was made possible by the generous financial support of the W.M. Keck Foundation. The authors wish to recognize and acknowledge the very significant cultural role and reverence that the summit of Mauna Kea has always had within the indigenous Hawaiian community. We are most fortunate to have the opportunity to conduct observations from this mountain.

REFERENCES

- Allen, M. M., Jenkins, E. B., & Snow, T. P. 1992, *ApJS*, 83, 261
- Cartledge, S. I. B., Lauroesch, J. T., Meyer, D. M., & Sofia, U. J. 2004, *ApJ*, 613, 1037
- de Avillez, M. A. & Mac Low, M.-M. 2002, *ApJ*, 581, 1047
- Draine, B. T. 2004, in *Origin and Evolution of the Elements*, ed. A. McWilliam & M. Rauch (Cambridge: Cambridge Univ. Press), 320
- Draine, B. T. 2006, in *proceedings of Astrophysics in the Far Ultraviolet: Five Years of Discovery with FUSE ASP Conference Series*, Eds G. Sonneborn, H. Moos, and B-G Andersson, 348, 58
- Friedman, S. D., et al. 2002, *ApJS*, 140, 37
- Gondhalekar, P. M., 1985, *ApJ*, 293, 230
- Hébrard, G., et al. 2002, *ApJS*, 140, 103
- Hébrard, G., Friedman, S. D., Tripp, T. M., Chayer, P., Lecavelier des Etangs, A., Oliveira, C. M., Moos, H. W., Vidal-Madjar, A., 2005a, *Bulletin of the American Astronomical Society*, 37, 1446
- Hébrard, G., Tripp, T. M., Chayer, P., Friedman, S. D., Dupuis, J., Sonnentrucker, P., Williger, G. M., Moos, H. W., 2005b, *ApJ*, 635, 1136
- Hoopes, C. G., Sembach, K. R., Hébrard, G., Moos, H. W., & Knauth, D. C. 2003, *ApJ*, 586, 1094
- Holweger, H., 2001, in *Solar and Galactic Composition*, ed. R. Wimmer-Schweingruber, (Berlin: Springer), 23
- Hunter, I., Smoker, J. V., Keenan, F. P., Ledoux, C., Jehin, E., Cabanac, R., Melo, C., Bagnulo, S., 2006, *MNRAS*, 367, 1478
- Jenkins, E. B., 2004, in *Origin and Evolution of the Elements*, ed. A. McWilliam & M. Rauch (Cambridge: Cambridge Univ. Press), 336.
- Jenkins, E. B., Tripp, T. M., Wozniak, P. R., Sofia, U. J., & Sonneborn, G. 1999, *ApJ*, 520, 182
- Jura, M. 1982, in *Advances in UV Astronomy: 4 Years of IUE Research*, ed. Y. Kondo, J. M. Mead, & Chapman, R. D. (NASA CP 2238; Greenbelt MD: NASA), 54
- Keller, L. P., Messenger, S., & Bradley, J. P. 2000, *J. Geophys. Res.*, 105, 10397
- Kirkman, D., Tytler, D., Suzuki, N., O'Meara, J. M., Lubin, D., 2003 *ApJS*, 149, 1
- Knauth, D. C., Meyer, D. M., Lauroesch, J. T., 2006, 647, L15
- Laurent, C., Vidal-Madjar, A., & York, D. G. 1979, *ApJ*, 229, 923
- Lacour, S., André M. K., Sonnentrucker, P., Le Petit, F., Welty, D. E., Desert, J.-M., Ferlet, R., Roueff, E., York, D. G., 2005, *A&A*, 430, 967
- Linsky, J. L., 2006, *ApJ*, 647, 1106
- Liszt, H. S., 2006, *A&A*, 452, 269
- Lodders, K., 2003, *ApJ*, 591, 1220

- Meyer, D. M., Jura, M., & Cardelli, J. A. 1998, *ApJ*, 493, 222
- Moos, H. W. et al. 2002, *ApJS*, 140, 3
- Oliveira, C. M., Dupuis, J., Chayer, P., & Moos, H. W. 2005, *ApJ*, 625, 232
- Oliveira, C. M., Hebrard, G., 2006, *ApJ*, 653, 345
- Oliveira, C. M., Moos, H. W., Chayer, P., & Kruk, J. W. 2006, *ApJ*, 642, 283
- O'Meara, J. M., Tytler, D., Kirkman, D., Suzuki, N., Prochaska, J. X., Lubin, D., Wolfe, A. M., 2001, *ApJ*, 552, 718
- Pan, K., Federman, S. R., Cunha, K., Smith, V. V., Welty, D. E., 2004, *ApJS*, 151, 313
- Pettini, M., 2006, in proceedings of Astrophysics in the Far Ultraviolet: Five Years of Discovery with FUSE ASP Conference Series, Eds G. Sonneborn, H. Moos, and B-G Andersson, 348, 19
- Pettini, M. & Bowen, D. V., 2001, *ApJ*, 560, 41
- Phillips, A. P., Gondhalekar P. M., & Pettini, M., 1982, *MNRAS*, 200, 687
- Prochaska, J. X., Tripp, T. M., & Howk, J. C. 2005, *ApJ*, 620, L39
- Redfield, S., & Linsky, J. L., 2002, *ApJS*, 139, 439
- Romano, D., Tosi, M., Chiappini, C., & Matteucci, F. 2006, *MNRAS*, 369, 295
- Savage, B. D., & Bohlin, R. C., 1979, *ApJ*, 229, 136
- Savage, B. D., Lehner, N., Fox, A., Wakker, B., Sembach, K., 2007, *ApJ*, accepted, astro-ph/0701110
- Savage, B. D. & Sembach, K. R., 1996, *ARA&A*, 34, 279
- Sembach, K. R., et al. 2004, *ApJS*, 150, 387
- Sonneborn, G., Tripp, T. M., Ferlet, R., Jenkins, E. B., Sofia, U. J., Vidal-Madjar, A., & Wozniak, P. R. 2000, *ApJ*, 545, 277
- Sonneborn, G., et al. 2002, *ApJS*, 140, 51
- Spitzer, L. 1985, *ApJ*, 290, L21
- Steigman, G., Romano, D., Tosi, M., 2007, *MNRAS*, accepted, arXiv:0704.0550v1
- Tielens, A. G. G. M. 1983, *A&A*, 119, 177
- van Steenberg, M. E. & Shull, J. M. 1988, *ApJS*, 67, 225
- Vidal-Madjar, A., Laurent, C., Bonnett, R. M., & York, D. G. 1977, *ApJ*, 211, 91
- Welsh, B. Y., Sasseen, T., Craig, N., Jelinsky, S., Albert, C. E., 1997, *ApJS*, 112, 507
- Wood, B. E., Linsky, J. L., Hébrard, G., Williger, G. M., Moos, H. W., & Blair, W. P. 2004, *ApJ*, 609, 838
- York, D. G. & Rogerson, J. B. 1976, *ApJ*, 203, 378